JSEE Vol. 25, No. 1&2, 2023 DOI: 10.48303/jsee.2023.1999067.1055

Research Paper

A Comprehensive Probabilistic Seismic Hazard Analysis of Karaj, Iran Using Classical and Monte Carlo Simulation Approaches

Mina Rashidirad[1], Nazila Kheirkhah[2] and Erfan Firuzi[3*]

1.M.Sc. Graduate, International Institute of Earthquake Engineering and Seismology (IIEES), Tehran, Iran
2. M.Sc. Graduate; Institute of Geophysics, University of Tehran, Tehran, Iran
3. Assistant Professor, Structural Engineering Research Center, International Institute of Earthquake Engineering and Seismology (IIEES), Tehran, Iran,
*Corresponding Author; email: e.firuzi@iiees.ac.ir

Received: 27/03/2023
Revised: 17/07/2023
Accepted: 02/09/2023

ABSTRACT

This study provides a comprehensive probabilistic seismic hazard assessment for Karaj, the capital of Alborz province. In the present study, two probabilistic approaches, including the classical and Monte Carlo methods are applied. In this regard, the most recent earthquake catalog of the region, as well as, the most appropriate GMPEs based on the statistical tests of the likelihood and the log-likelihood are used. The results indicated that there are differences between the results of two approaches, which is intensified in the longer return periods. This disparity mainly stemmed from the different concept of two methods for incorporating the aleatory uncertainty. In the classical PSHA, the aleatory uncertainty takes into account using the integration, which is truncated at a fixed number of the logarithmic standard deviation. While, in the Monte Carlo simulation approach, the aleatory uncertainty is considered in calculation using random sampling of GMPEs variability. In addition, the ground motion shaking map of the region for the dominant seismic scenarios, including the rupture of the North-Tehran and Eshtehard faults are developed. These seismic scenarios have the potential of producing the greatest acceleration; consequently, the most vulnerability. The outcomes of this study can be used for providing urban plan or estimating the probable economic and casualty losses of Karaj.

Keywords:
Probabilistic seismic hazard assessment; Classical seismic hazard Analysis; Monte Carlo simulation; Karaj; Iran

1. Introduction

Located in the north central of Iran, Karaj is the capital of Alborz province. Karaj's population has grown dramatically in recent decades. According to the Statistical Center of Iran (SCI), the total population of Karaj was 14,526 in the first national census in 1966, but it has since climbed to almost 1.97 million in the 2016 census. This is Iran's fourth most populous city, after Tehran, Mashhad and Isfahan. With a total area of 1419 km^2, this city also has the greatest population density of all the cities in Iran (SCI, 2016). Along with its demographic characteristics, Karaj contributes more than 3% of the country's Gross Domestic Product (GDP) and is rated 10th among Iran's provinces. Additionally, this is the most important city in the proximity of Tehran, the capital of Iran, which can play a key role in response of occurring natural disaster in Tehran. As a result, the government is substantially concerned about Karaj safety from natural risks.

Earthquake is one of the most serious threats of natural disasters in Karaj. Tectonically, the city located at the southern edge of the Alborz Mountains. The region is identified by their shallow large earthquakes (Berberian & Yeats, 1999). As shown in Figure 1, the city also lied at the Central-East Iran seismotectonic province defined by Mirzaei et al. (1998). This is a high seismic prone region due to the compressive stress by Arabia-Eurasia Convergence (Jackson et al., 2000). There are several active seismic faults in this tectonic setting including North-Tehran Fault (NFT), Mosha, Eshtehard and Taleghan (Ashtari et al., 2005). Figure (1) shows the boundary of Karaj with respect to the active faults in a radius of 150 km. It shows the distribution of historical earthquakes, as well. The last strong earthquake in Karaj occurred in 1830. By considering time interval of strong earthquakes, there is a high probability of occurring a great earthquake in near future in Karaj (Jalalalhosseini et al., 2018).

Alongside the high seismicity of the region, the high vulnerability of built-environment results in Karaj's high seismic risk. This issue reflected the importance of conducting a detailed seismic risk assessment to address the impact of earthquakes in the region. The first step for conducting seismic risk assessment is performing seismic hazard analysis. Therefore, the main purpose of this study is providing a comprehensive seismic hazard model for Karaj.

There are two common approaches for Probabilistic Seismic Hazard Assessment (PSHA) in a region: 1) the classical method, and 2) the Monte Carlo simulation (event-based) method. In the classical approach, the annual rate of occurring different ground motion values, which called "hazard curve", is estimated according to the approach developed by Cornel (1968). This approach formed on the basis of total probability theorem. In this approach, the hazard curve is derived from aggregating all potential seismic sources by con-sidering their corresponding seismicity. Thus, their results typically associated with conservative. In the event-based approach, the hazard curve is obtained from assessing the impact of hundreds of synthetic catalogs with the length of thousands years (Ebel & Kafka, 1999; Musson, 2000). This is a useful tool to capture epistemic and aleatory uncertainties in PSHA (Ansari et al., 2015). Determining the priority for using each of these methods depends on the

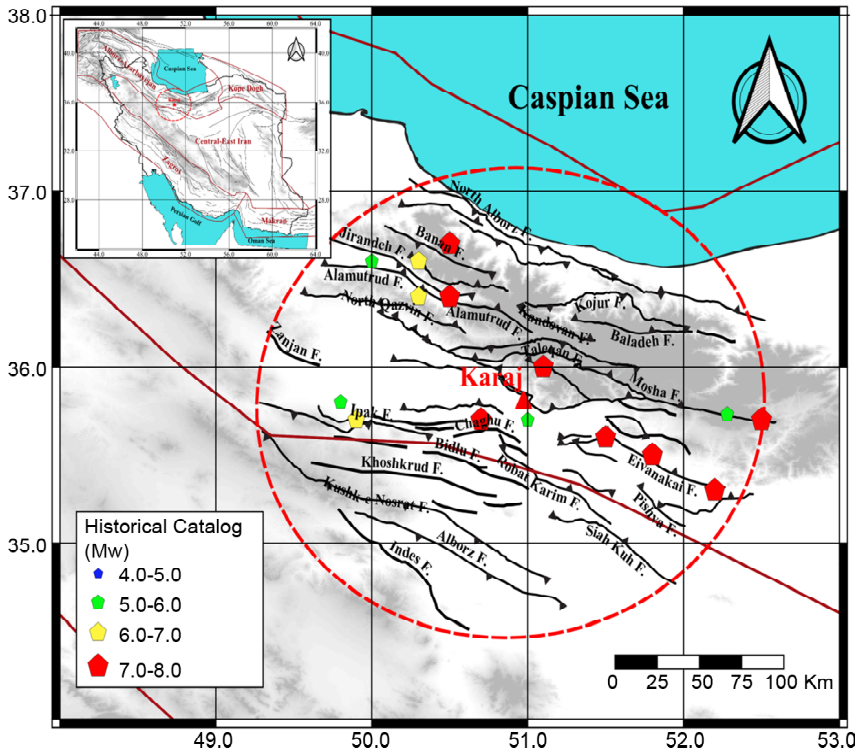

Figure 1. Distribution of active faults and historical events in radius of 150 km around Karaj (red lines are the seismotectonic provinces defined by Mirzaie et al. (1998)).

application. The classical PSHA analysis is generally used for providing a comparing hazard map across a region. While, the event-based approach is employed when the mean and variation of results are important (Crowley, 2014). In the event-based approach, the impact of earthquakes separately considered in the analysis; therefore, it is possible to provide a probability distribution of outcomes. In the present study, the seismic hazard analysis on the region is estimated using both approaches.

While several studies in the literature assessed the seismic hazard in Iran or Tehran as the capital of Iran; only few studies evaluated the seismic hazard in Karaj. Jarahi (2016) performed a classical PSHA to determine dominant earthquakes for the design-basis earthquake level in Karaj (i.e., 10 percent probability of occurrence in 50 years). He performed analysis using EZ-FRISK program with a log tree composed of 120 branches. Jarahi (2016) results show a range of Peak Ground Acceleration (PGA) of 0.45-0.60 g on firm rock in Karaj, which is significantly higher than the suggested value by the national Iranian building code, 0.35 g (Standard 2800). Jalalalhosseini et al. (2018) performed a time-depended seismic hazard analysis for Greater Tehran and surrounding area.

This analysis is performed using a smooth seismicity model. They report the value of PGA for return period of 475 years in Karaj about 0.35-0.42g. Zaman and Ghayamghamian (2021), as a part of their study for evaluating risk adjusted map for Karaj, performed a classical PSHA. To quantify seismic hazard, they used eight GMPEs and one seismic source model. Their results show a range of 0.3-0.45 g for PGA on bed-rock for return period of 475 years in Karaj. In addition to aforementioned studies, there are also some national or regional seismic hazard assessment, the most recent one is Earthquake Model of Middle East project (EMME). This project is performed by cooperation researches from 11 countries in last four years. Danciu et al. (2018) comprehensively describe the calculation procedure in the EMME project.

This seismic source model in the EMME project composed of an area source model, a fault model and a background seismicity model. In addition, four GMPEs for shallow tectonic region are employed, and OpenQuake software is used for the analysis (Pagani et al., 2014). The results of this study report the value of PGA on bed-rock in Karaj about 0.4 g.

Review of aforementioned studies show previous studies used the classical PSHA approach to quantify the seismic hazard in Karaj. To the author knowledge, there are no studies in literature that employed the event-based or Monte Carlo approach for seismic hazard analysis. These methods, which are based on seismic scenarios, are more applicable for seismic risk assessment (Firuzi et al., 2019, Crowley, 2014). Thus, the primary goal of this study is to estimate seismic hazard in Karaj based on all aforementioned approaches to provide a comprehensive seismic hazard model, which can be used for seismic risk assessment. It should be mentioned that aforementioned approaches are probabilistic methods, which generally lead to lose of the hazard due to the most vulnerable seismic scenario. Thus, in the present study, the ground motion shaking maps of the region is also developed for dominant seismic scenarios of Karaj. In the following, first, the procedure to compile the earthquake catalog and its related analysis is presented. Then, the process of selecting the most appropriate Ground Motion Prediction Equations (GMPEs) for the region of interest is introduced. Next, the results of seismic hazard in Karaj using the classical PSHA approach are presented, together with a comprehensive discussion about the available uncertainties in analysis. Subsequently, the seismic hazard in Karaj by implementing the event-based approach is provided, with a detailed comparison between the results of approaches.

Finally, the ground motion shaking map of Karaj for dominant seismic scenarios are developed. The outputs of seismic hazard map in this study can be used for estimating seismic risk assessment.

2. Compiling Earthquake Catalog

The earthquake catalog is used in both classical and event-based PSHA analysis. Thus, compiling a reliable and homogenous earthquake catalog is an important step in SHA. In the present study, the

earthquake catalog compiled by Mousavi-Bafrouei and Mahani (2020) is used to extract the events within a radius of 150 km around Karaj. Mousavi-Bafrouei and Mahani (2020) compiled the earthquake catalog from data of local and international agencies. However, this catalog covers events till December 31, 2018. In the present study, recent earthquakes added to the catalog using information provided by Iranian Seismological Center (IRSC). IRSC is the official center responsible for reporting earthquakes data in Iran. IRSC provides the earthquake catalog on MN scale. Thus, the relation provided by Mousavi-Bafrouei and Mahani (2020) is used to homogenize the earthquake catalog. The final instrumental earthquake catalog is composed of 711 events with magnitude greater than 3.0 Mw to the end of June 2022. Figure (2) shows the distribution of the events in a 150-kilometer radius surrounding Karaj. The maximum curvature approach is adopted to determine the catalog's completeness. This method implemented in the ZMAP package, which was developed for the statistical analysis of seismic data (Wiemer, 2001). Table (1) summarizes the catalog's completeness. The results show good consistency with analysis of Khodaverdian et al. (2016), which assessed the completeness of earthquakes in Iran. The time-space window approach proposed by Gardner and Knopoff (1974) and the cross-correlation method developed by Reasenberg (1985) are used for declustering the earthquake catalog. The former identifies 541 events as independent events; while the latter identifies 633 events as main earthquakes. These catalogs are used for estimating the seismicity parameters and generating synthetic catalog in following sections.

Table 1. The completeness magnitude of the compiled earthquake catalog.

Time Window	Magnitude (Mw)
1930-1965	5.5
1965-1990	4.5
1990-2005	4.0
2005-2022	3.5

3. Selecting Appropriate GMPEs

GMPEs provide an estimation of the engineering parameters such PGA and spectral acceleration as a function of factors like magnitude, distance, and site conditions. It should be noted that GMPEs are proxy-models and associated with lots of uncertainties (Fallah Tafti et al., 2017). Thus, it is important to properly consider their variabilities in

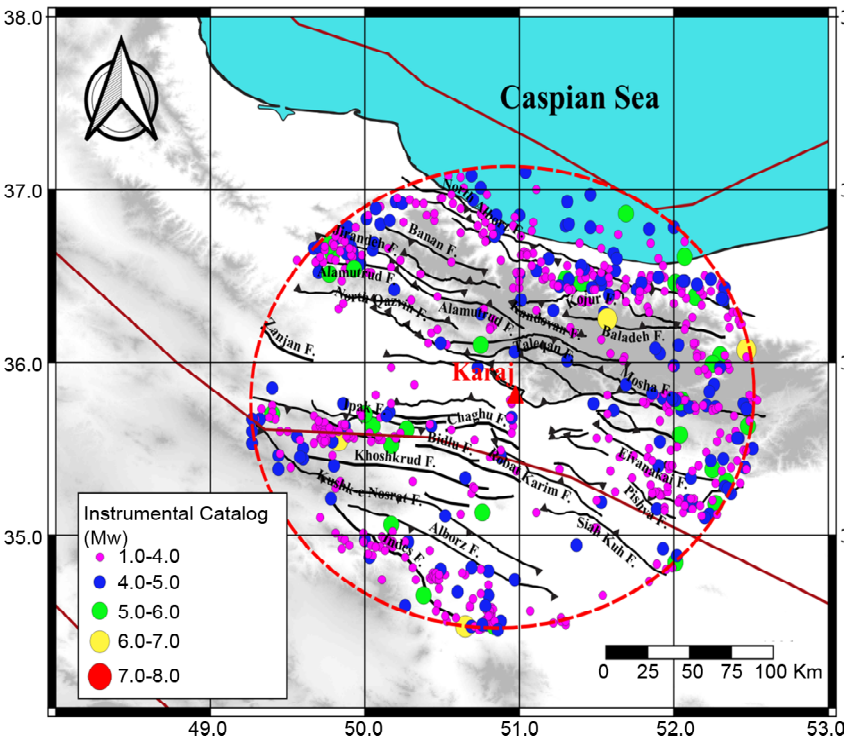

Figure 2. Distribution of instrumental earthquakes in a radius of 150 km around Karaj.

analysis. To incorporate the epistemic uncertainty of GMPEs from subjective opinion of the analyst, the logic tree is used (Firuzi et al., 2019).

In this study, for assessing the suitability of GMPEs, two statistical tests including the likelihood (LH), and log likelihood (LLH) proposed by Scherbaum et al. (2004, 2009) are used. These methods evaluate the potential of GMPEs to capture observed ground motion values in the past earthquake of region. These methods employed in several studies such as Mousavi et al. (2012), Zafarani and Mousavi (2014) and Firuzi et al. (2020) for selecting and ranking of GMPEs. Table (2) lists the main characteristics of nine candidate GMPEs, the performance of which assessed in the present study. It should be remarked that majority of candidate models meet the criteria provided by Cotton et al. (2006) and Bommer et al. (2010). For example, Idriss (2014), which is one of the relations of NGA-WEST2 project, does not include in the candidate GMPEs since it does not cover the soft soil.

The high-quality database of strong ground motion compiled by Zafarani and Soghrat (2017) is used for statistical tests. The final database is composed of 156 three-component records from 30 earthquakes around Karaj. It should be noted that for stations in which the VS30 is not available, the H/V approach proposed by Ghasemi et al. (2009) is used to have an estimation of the soil class. Beauval et al. (2012) stated that the minimum number of records for statistical tests of GMPEs is about 40 records. Thus, it is believed that our database is rich enough to provide stable results. Figure (3) shows the distribution of selected earthquakes for evaluating GMPEs performance.

The analysis is performed in four periods including PGA, 0.1, 0.5 and 1.0 second. Based on the LH values, the central tendency and variability of the normalized residual, Scherbaum et al. (2004) rank GMPEs in four groups (A to D), with A representing the best performance and D representing the poor performance. The LLH approach uses the information theory for ranking of GMPEs (Scherbaum et al., 2009). In this method, the lower value of LLH shows the better performance. The result of analysis in different periods is provided in Table (3).

As presented, the relations of Fetal19, Zetal18, Bietal14, Aetal14 and Betal14 show the best performance in both approaches. These relations, which are ranked among the top five are used in logic tree with equal weights. It should be noted that the North-Tehran Fault passes through Karaj. Thus, near-field effects such as velocity pulses or directivity should be considered in the analysis. The most relevant approach for taking into account such impacts in analysis is using complicated GMPEs like NGA-west2 models in the analysis.

Table 2. The main characteristics of candidate GMPEs.

GMPE	Abbreviation	Region	Magnitude (M_w)	Distance Metric (Km)	Period Range	Site Effect
Farajpour et al. (2019)	Fetal19	Iran	4.8-7.5	0-400 (R_{rup})	0.0-4.0	V_{S30}
Zafarani et al. (2018)	Zetal18	Iran	4.0-7.3	0-200 (R_{jb})	0.0-4.0	Dummy Variable (4)
Kotha et al. (2016)	Ketal16	Middle East	4.0-7.6	0-200 (R_{jb})	0.0-4.0, PGV	V_{S30}
Kale et al. (2015)	Ketal15	Iran + Turkey	4.0-8.8	0-200 (R_{jb})	0-4.0, PGV	V_{S30}
Bindi et al. (2014)	Bietal14	Europe and Middle East	4.0-7.6	0-300 (R_{jb})	0-3.0, PGV	Dummy Variable (4)
Campbell and Bozorgnia (2014)	CB14	Global Data with Concentration on California	3.0-7.9	1-300 (R_{rup})	0-10 (PGV)	V_{S30}
Boore et al. (2014)	Betal14	Global Data with Concentration on California	3.0-7.9	0-400 (R_{rup})	0-10 (PGV)	V_{S30}
Chiou and Youngs (2014)	CY14	Global Data with Concentration on California	3.5-7.9	1-300 (R_{rup})	0-10 (PGV)	V_{S30}
Abrahamson et al. (2014)	Aetal14	Global Data with Concentration on California	3.0-7.9	0-400 (R_{rup})	0-10, PGV	V_{S30}

These GMPEs typically have terms such as directivity and hanging-wall which include the near source effect in the analysis. In the present study, two of selected GMPEs (i.e., Aetal14 and Betal14) are from NGA-west2, which include the near-fault effects in analysis.

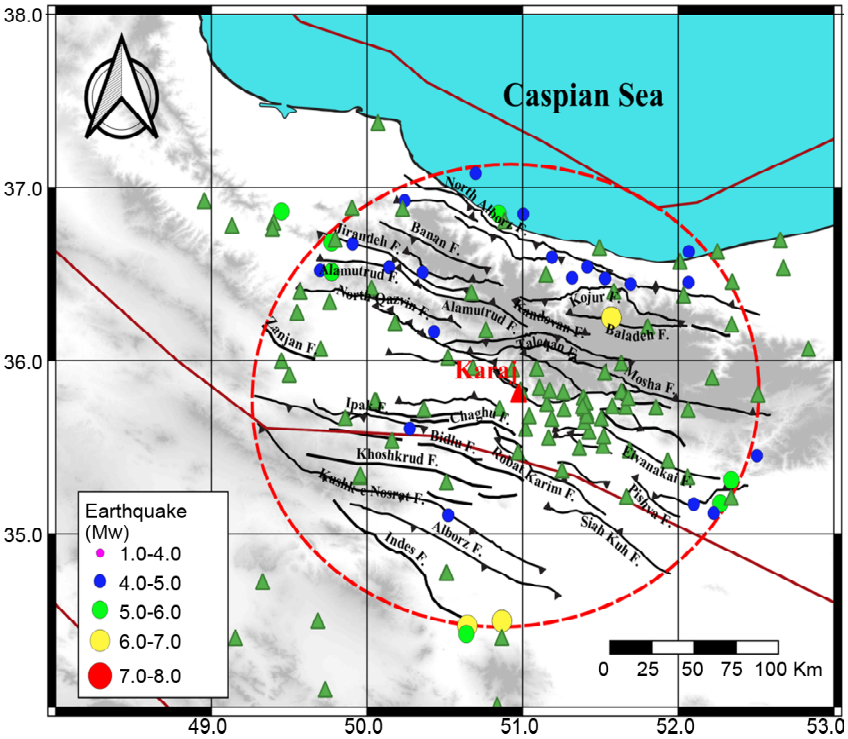

Figure 3. Distribution earthquakes and seismic stations in strong ground motion database for assessing appropriate of candidate GMPEs (green triangles are seismic stations operated by ISMN (Iranian Strong Ground Motion Network)).

Table 3. The median, mean and standard deviation of normalized residual with corresponding rank based on the LH proposed by Scherbaum et al. (2004) and LLH values in different periods.

Att. Relation	MEDLH	MEDNR	MEANNR	STDNR	RANK	LLH	Att. Relation	MEDLH	MEDNR	MEANNR	STDNR	RANK	LLH
			T = 0 sec							T = 0.1 sec			
CB14	0.33	-0.45	-0.26	1.18	B	1.73	CB14	0.34	-0.66	-0.49	1.18	B	2.03
Betal14	0.47	-0.13	0.12	1.17	B	1.69	Betal14	0.41	-0.32	-0.21	1.15	B	1.87
CY14	0.40	-0.33	-0.01	1.26	C	1.79	CY14	0.40	-0.52	-0.38	1.15	B	1.97
Aetal14	0.43	-0.33	-0.20	0.99	A	1.55	Aetal14	0.38	-0.58	-0.47	1.07	B	1.83
Ketal15	0.54	-0.26	0.06	1.06	A	1.54	Ketal15	0.55	-0.21	-0.08	1.03	A	1.60
Ketal16	0.49	-0.36	-0.22	0.89	A	1.24	Ketal16	0.48	-0.51	-0.52	0.91	A	1.54
Bictal14	0.63	0.08	0.26	0.95	B	1.58	Bictal14	0.61	-0.07	0.01	0.88	A	1.56
Zctal18	0.62	-0.16	0.02	0.67	A	1.11	Zctal18	0.61	-0.22	-0.21	0.73	A	1.33
Fetal19	0.70	-0.20	-0.16	0.50	A	1.12	Fetal19	0.67	-0.07	-0.03	0.54	A	1.34
			T = 0.5 sec							T = 1 sec			
CB14	0.31	-0.92	-0.73	0.98	B	2.31	CB14	0.44	-0.62	-0.51	0.96	A	2.91
Betal14	0.35	-0.78	-0.58	1.05	B	2.22	Betal14	0.48	-0.39	-0.31	1.01	A	2.80
CY14	0.37	-0.72	-0.55	1.00	B	2.19	CY14	0.49	-0.43	-0.31	0.97	A	2.82
Aetal14	0.38	-0.75	-0.63	0.88	B	2.13	Aetal14	0.53	-0.38	-0.31	0.86	A	2.63
Ketal15	0.34	-0.92	-0.75	0.76	B	2.12	Ketal15	0.45	-0.67	-0.65	0.69	A	2.79
Ketal16	0.31	-1.01	-1.04	0.87	B	2.36	Ketal16	0.38	-0.84	-0.84	0.91	B	3.18
Bietal14	0.51	-0.49	-0.35	0.78	A	1.92	Bietal14	0.63	-0.17	-0.05	0.83	A	2.58
Zetal18	0.55	-0.58	-0.56	0.61	A	1.78	Zetal18	0.65	-0.38	-0.37	0.61	A	2.38
Fetal19	0.68	-0.01	-0.02	0.52	A	1.62	Fetal19	0.66	0.11	0.08	0.53	A	2.23

MEDLH: Median LH
MEANNR: Mean Normalized Residual
MEDNR: Medina Normalized Residual
STDNR: Standard Deviation Normalized Residual

4. Classical PSHA

This section provides a description of classical PSHA steps including defining seismic sources, assigning seismicity parameters and modeling uncertainties.

Delineating seismic sources is a subjective step in classical PSHA. Here, three seismic source models as depicted in Figure (4) are considered in analysis. In defining seismic source models factors such as seismic depth, fault trend, fault mechanism, seismotectonic provinces, past earthquakes and geological evidence are considered. In addition, a background seismicity model, consisting of a uniform grid cell of 0.1×0.1 degree, considered in the analysis. The approach proposed by Kijko and Sellevoll (1992), which considered the completeness of earthquake catalog in analysis, is used for estimating seismicity parameters. A short review of the most important seismic source parameters for line sources are presented in Table (4).

Capturing aleatory and epistemic variabilities in calculation is the other important step in classical PSHA. The aleatory viability stems from the randomness nature of earthquake. The epistemic uncertainty comes from factors like inaccuracy of

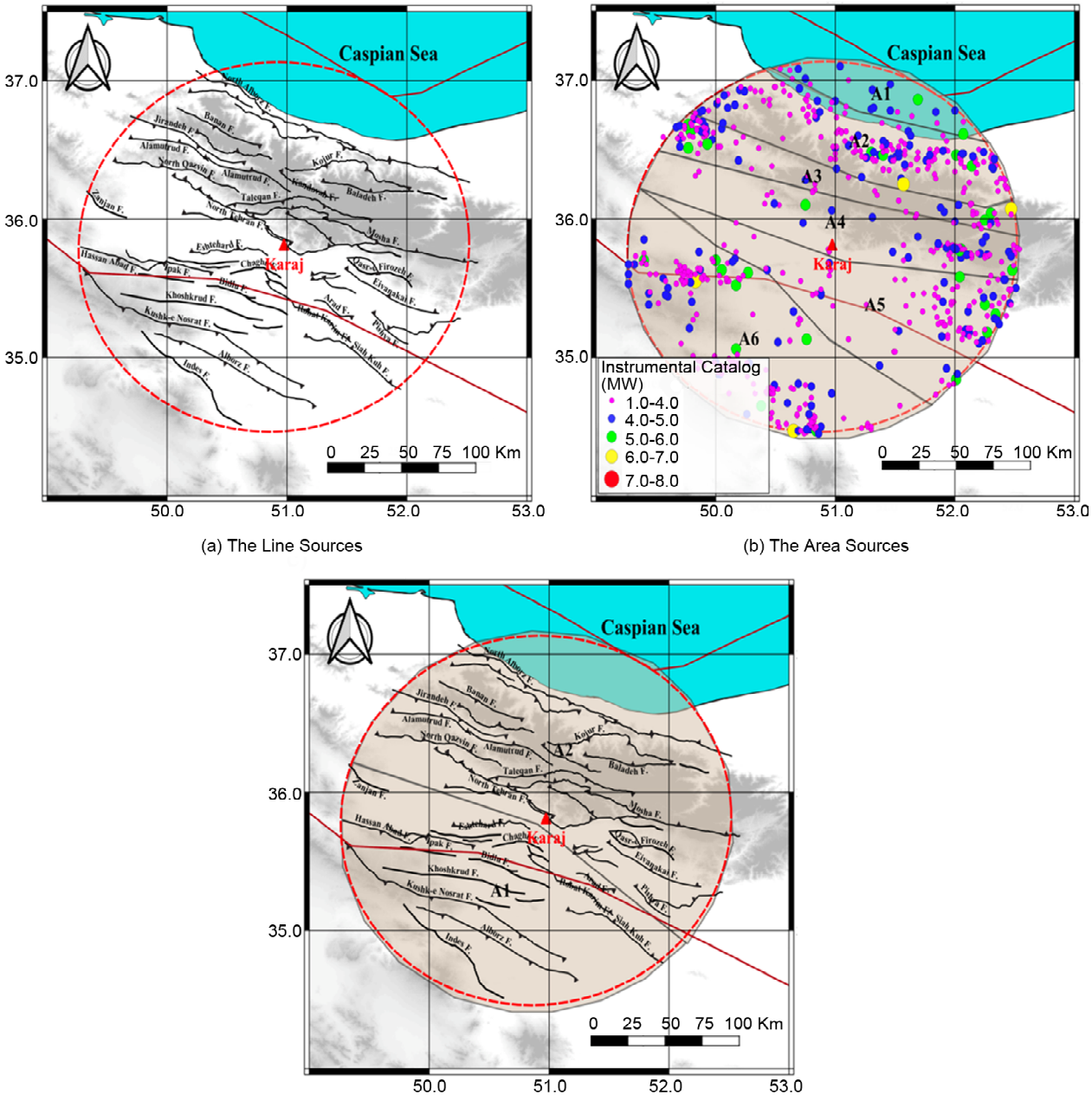

(a) The Line Sources

(b) The Area Sources

(c) Combination of Line Sources and Area Sources

Figure 4. Different seismic source models used in logic tree.

the model, incompleteness of data or subjective decisions by analyst. In the classical PSHA, the aleatory uncertainty captured in calculation using the total probability theorem. However, the epistemic uncertainty is considered in the analysis using logic tree (Bommer et al., 2005). Figure (5) illustrates the general structure of logic tree, which composed of 360 branches, employed in the present study.

Table 4. Review of the most important seismic source parameters of line sources for classical seismic hazard analysis.

No	Fault Name	Mmax1	Mmax2	Mmax3	a Value	b Value	Fault Type
1	Parandak F.	6.9	6.7	6.5	2.655	1.016	Unknown
2	Bidlu F.	6.9	6.8	6.6	2.707	1.016	Unknown
3	Norud F.	6.7	6.5	6.3	2.462	0.977	Unknown
4	Chaghu F.	7.0	6.8	6.6	2.737	1.016	Unknown
5	Qasr-e Firozeh F.	7.1	7.0	6.8	2.852	0.977	Unknown
6	Lirehsar F.	7.3	7.1	6.9	2.975	0.977	Reverse and Thrust
7	Emamzadeh Davoud F.	7.0	6.9	6.7	2.758	0.977	Reverse and Thrust
8	Eivanakai F.	7.3	7.1	7.0	3.003	0.977	Reverse and Thrust
9	Qeshlaq-Aladaghlu F.	7.0	6.8	6.6	2.724	0.977	Reverse and Thrust
10	Pishva F.	6.9	6.8	6.6	2.667	0.977	Reverse and Thrust
12	Indes F.	7.5	7.3	7.1	2.123	0.977	Reverse with Left Lateral Component
13	North of Rey F.	6.6	6.4	6.2	3.173	1.016	Reverse with Right Lateral Component
14	South of Rey F.	6.7	6.5	6.3	2.353	0.977	Reverse and Thrust
15	Garmsar F.	7.2	7.0	6.8	2.434	0.977	Reverse and Thrust
16	Kushk-e Nosrat F.	7.7	7.6	7.4	2.894	0.977	Reverse and Thrust
17	Mosha F.	7.7	7.6	7.4	3.422	1.016	Reverse with Left Lateral Component
18	Shour F.	6.6	6.5	6.3	3.401	0.977	Reverse with Left Lateral Component
19	Sariyal F.	6.7	6.5	6.3	2.451	1.016	Unknown
20	Khan Kish F.	6.7	6.5	6.3	2.457	1.016	Unknown
21	Sorkh-e Hessar	6.8	6.7	6.5	2.465	1.016	Unknown
22	Zard Rang F.	6.8	6.6	6.4	2.383	0.977	Reverse and Thrust
23	Siah Kuh F.	7.3	7.2	7.0	2.574	0.977	Reverse and Thrust
24	Eshtehard F.	7.2	7.0	6.8	2.548	1.016	Unknown
25	Ipak F.	7.2	7.1	6.9	2.186	0.977	Reverse with Left Lateral Component
26	Baladeh F.	7.2	7.1	6.9	2.340	0.977	Reverse with Left Lateral Component
27	Hassan Abad F.	7.2	7.1	6.9	3.071	1.016	Reverse and Thrust
28	Kandovan F.	7.1	6.9	6.7	2.921	1.016	Reverse and Thrust
29	Southern Galand Rud F.	7.2	7.0	6.8	2.981	1.016	Left Lateral
30	Jirandch F.	7.4	7.2	7.0	2.945	0.977	Reverse and Thrust
31	Kahrizak F.	6.8	6.6	6.4	2.963	1.016	Reverse and Thrust
32	Kojur F.	7.4	7.3	7.1	2.808	0.977	Reverse and Thrust
33	Suleh Sar F.	7.1	6.9	6.7	2.907	0.977	Reverse and Thrust
34	Zavardash F.	7.2	7.1	6.9	3.079	0.977	Reverse with Left Lateral Component
35	North Alborz F.	7.6	7.4	7.2	2.551	0.977	Reverse and Thrust
36	North Tehran F.	7.5	7.3	7.2	3.146	0.977	Reverse and Thrust
37	Alborz F.	7.6	7.4	7.2	2.805	0.977	Reverse and Thrust
38	North Qazvin F.	7.4	7.3	7.1	2.934	0.977	Reverse and Thrust
39	Taleqan F.	7.5	7.3	7.2	3.248	0.977	Reverse and Thrust
40	Zanjan F.	6.9	6.8	6.6	3.288	0.977	Reverse with Left Lateral Component
41	North Alborz F.	7.0	6.9	6.7	3.262	1.016	Reverse and Thrust
42	Khoshkrud F.	7.4	7.3	7.1	3.106	0.977	Reverse and Thrust
43	South Parandak F.	7.0	6.8	6.6	3.181	0.977	Reverse with Left Lateral Component
44	Robat Karim F.	7.3	7.2	7.0	2.700	1.016	Unknown
45	Arad F.	6.9	6.7	6.5	2.754	0.977	Reverse and Thrust
46	Alamutrud F.	7.2	7.1	6.9	3.166	1.016	Unknown
47	Alamutrud F.	7.2	7.0	6.8	2.853	1.016	Unknown
48	Banan F.	7.2	7.1	6.9	2.747	1.016	Unknown

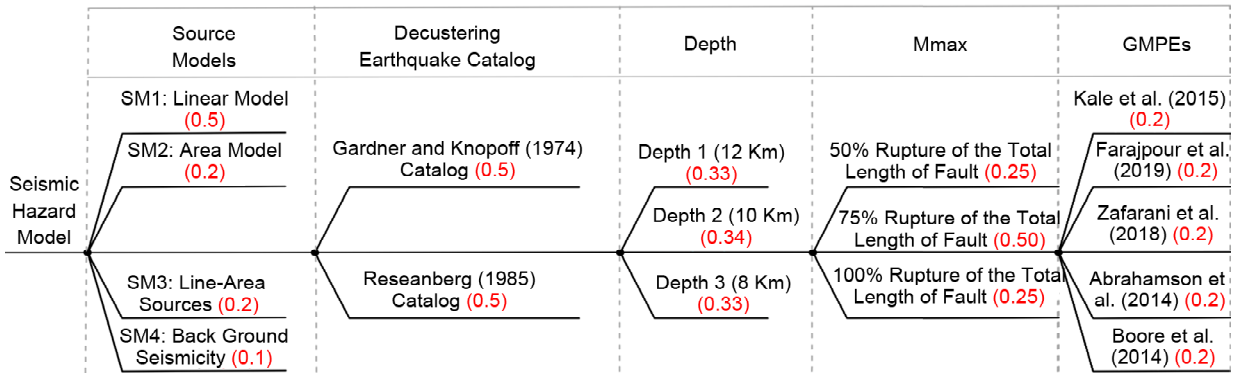

Figure 5. The general structure of logic tree used in the present study to quantify the seismic hazard using classical PSHA (red numbers are weights of branches).

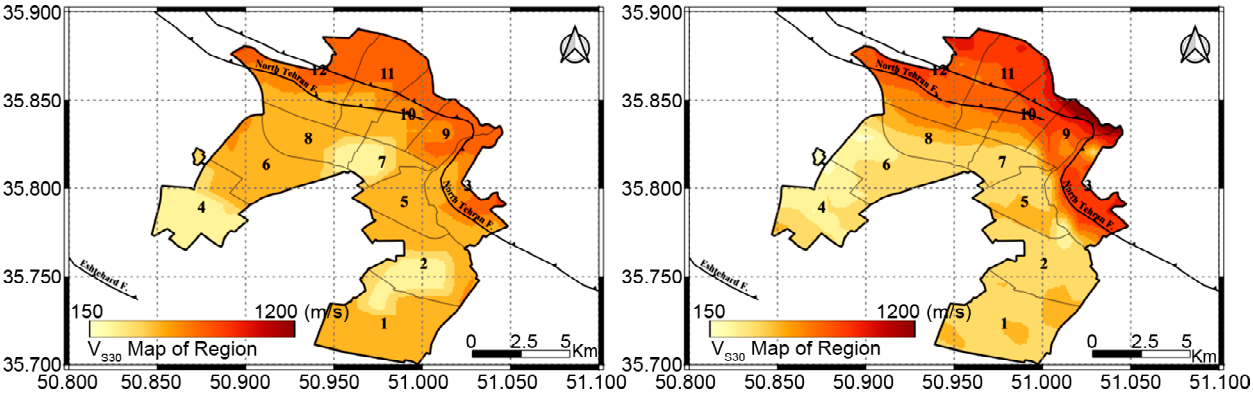

(a) IIEES (2013) (b) Wald and Allen (2007)

Figure 6. The general structure of logic tree used in the present study to quantify the seismic hazard using classical PSHA (red numbers are weights of branches).

The near-surface amplification was considered in calculation using the V_{S30} map of region. The V_{S30} map extracted from two different sources: 1) a microzonation study done by International Institute of Earthquake Engineering and Seismology (IIEES, 2013), and 2) topographic slope approach developed by Wald and Allen (2007). Figure (6) shows the V_{S30} map of Karaj using both methodologies. As depicted, there is a significant correlation between the results. In both approaches, the northern part of the city, near the foothill of Alborz Mountains, has higher V_{S30}; while, the southern part of the city has lower V_{S30}. In the present study, both approaches considered in analysis using logic tree with equal weights.

The OpenQuake software, which is becoming a routine in PSHA, is used for quantifying the seismic hazard in the present study. This is an open-source software, which has appropriate flexibility in employing the logic tree (Pagani et al., 2014). Figure (7) shows the seismic hazard map of Karaj within 12 municipal districts in return periods of 475 and 2475 on engineering bed-rock and soil surface. As depicted, the north-west of Karaj has the highest acceleration on bed-rock (i.e., district number 6, 8, 11 and 12). This is due to the active North-Tehran Fault. By employing the local site condition, the acceleration in the south-west and central parts of the city is increased (i.e., district number 2, 4, 7 and 8). The presence of soft soil in these areas is the main reason for such acceleration increment.

5. Event-Based PSHA

Although the classical PSHA approach is widely used by the engineering community for seismic hazard assessment, results of this method are highly dependent on the opinion of the analyst. In cases, the results of classical PSHA for a region in different studies show significant variation. For example, Jarahi (2016) reports PGA on bed-rock for Karaj in the range of 0.45-0.60 g,

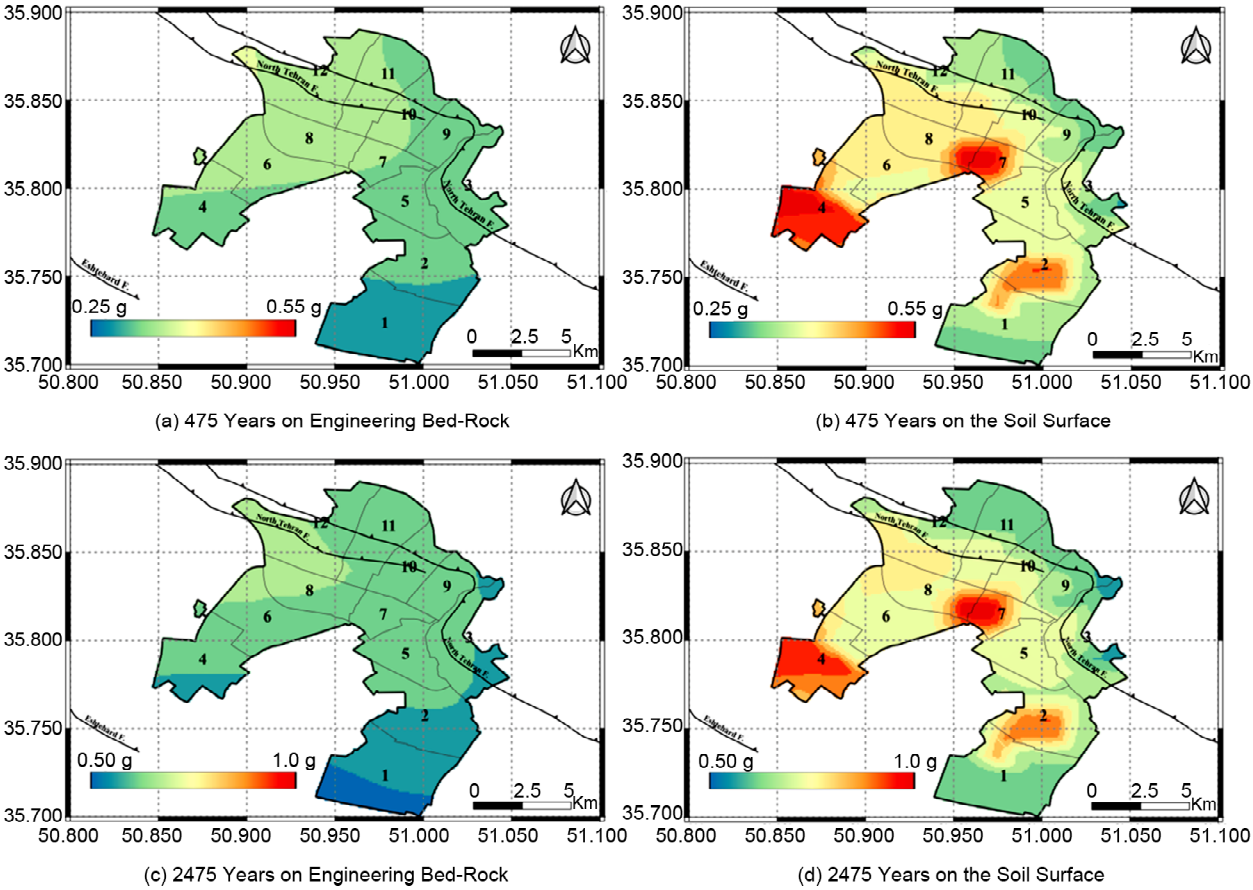

Figure 7. The seismic hazard map of Karaj using classical approach (PGA) for return periods.

while the current study or Jalalhosseini et al. (2018) report PGA on bed-rock in the range of 0.35-0.45 g for the same return period. This discrepancy generally stems from subjective decision of analysts on defining seismic sources and assigning seismicity parameters. To address this shortcoming, event- based or Monte Carlo simulation tool is introduced. The approach can be considered as an appropriate method to eliminate all aforementioned subjectivity in PSHA (Ebel & Kafka, 1999; Musson, 2000). In addition, capturing uncertainties like spatial correlation in the classical approach is thus difficult in comparison to Monte Carlo simulation method.

The underlying concept of Monte Carlo simulation method is generating random variables according to specific data or models to estimate the possible outcomes of an uncertain problem. In this method, hundreds of synthetic catalogs spanning thousands of years are generated at the region. Ebel and Kafka (1999), Han and Choi (2008), Musson (2000) and Ansari et al. (2015) proposed different algorithms for generating synthetic catalog. All of them follow the typical procedure illustrated in Figure (8). As depicted, first, epicenters of synthetic events are determined. Second, the magnitude of synthetic events added to the catalog. Next, the impact of synthetic events on the site of interest is evaluated. Finally, the annual rate of the occurrence, derived from the ground motion values of synthetic events and length of catalog. All of the aforementioned steps can be done using a specific data or a probabilistic model.

In the present study, the approach proposed by Ebel and Kafka (1999) is employed for generating the epicenter of synthetic events. In this method, epicenter of synthetic events is determined from the observed earthquakes by adding some variability based on a circular Gaussian probability density function, with radius of 30 km, centered the observed event. Magnitude of synthetic events is sampled from DCF of doubly Gutenberg-Richter relation (Gutenberg-Richter, 1994). The parameters of the area source model delineated in Figure (4b) are used for determining the CDF of

doubly Gutenberg-Richter relation. Figure (9) shows the observed earthquake catalog with a synthetic catalog with length of 250 years. As depicted, there is appropriate consistency between the observed catalog and the simulated catalog.

GMPEs are used for evaluating ground motion value of synthetic events at sites. The Monte Carlo simulation approach has appropriate flexibility in capturing the aleatory uncertainties. The aleatory uncertainty of GMPEs considered in the analysis by random sampling of GMPEs uncertainties. Total variability of GMPE is classified into: 1) the inter-event, and 2) intra-event variabilities. The inter-event attributed the uncertainty from one earthquake to another, while intra-event comes from variability from one site to another (Crowley & Bommer, 2006; Silva, 2017). Thus, inter-event variability is sample for each synthetic event. However, the intra-event uncertainty sampled in each site. To consider the spatial correlation in calculation, the intra-event variability coefficients should be select from a correlation model. In the present study, the model proposed by Zafarani et al. (2021) is adopted for generating the spatial intra-event variability coefficients. Zafarani et al. (2021) by compiling a reliable database of Iranian strong ground motion developed a spatial correlation model. In this model, the correlation between spatially distributed ground motions shaking is exponentially decreased by increasing the distance between assets.

To provide stable results in Mote Carlo simulation, appropriate number of iterations should be performed. In the present, 250 synthetic catalogs with the length of 100,000 are generated. This is the recommended value proposed by Silva (2017)

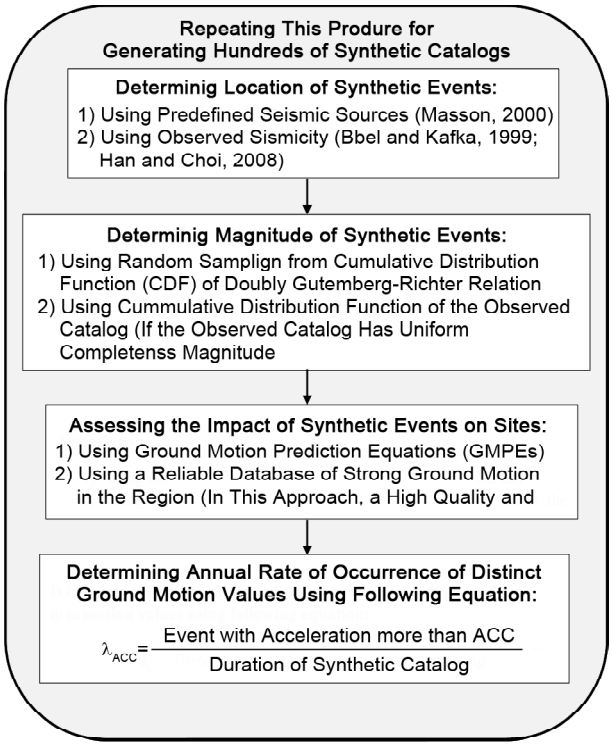

Figure 8. The general procedure of performing PSHA using Monte Carlo simulation approach.

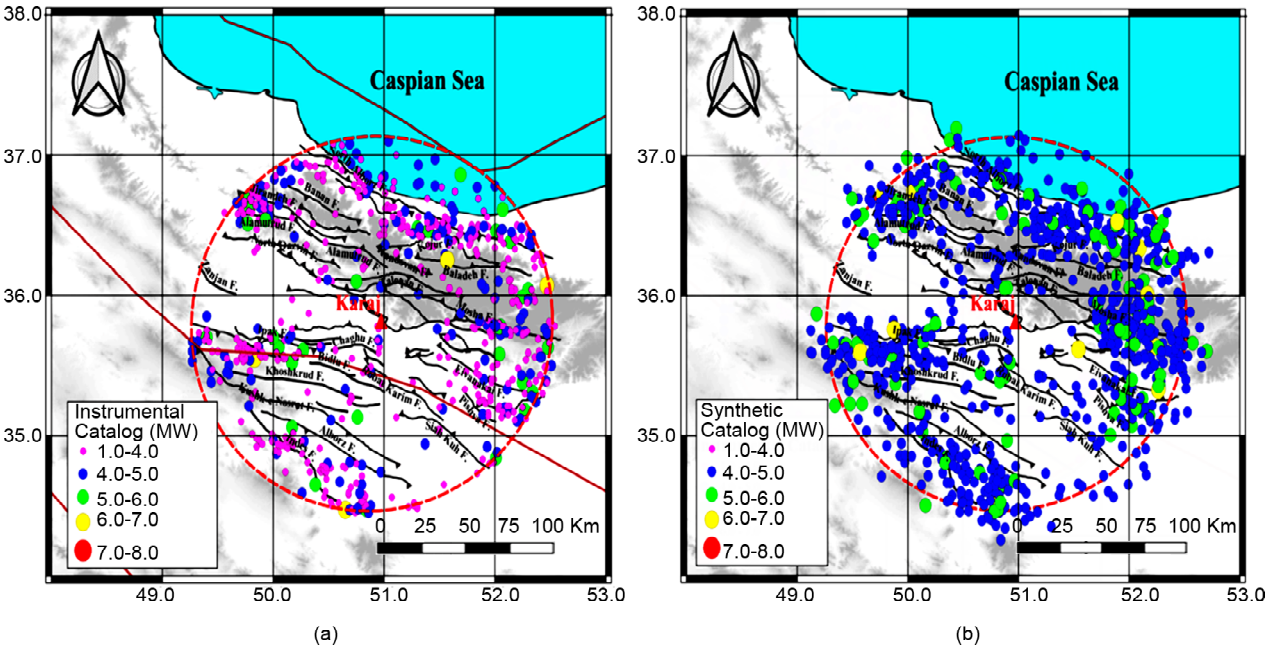

Figure 9. (a) the observes earthquake catalog of region with length of 120 years and (b) a sample of synthetic earthquake catalog of region generated using Monte Carlo simulation approach with length of 250 years.

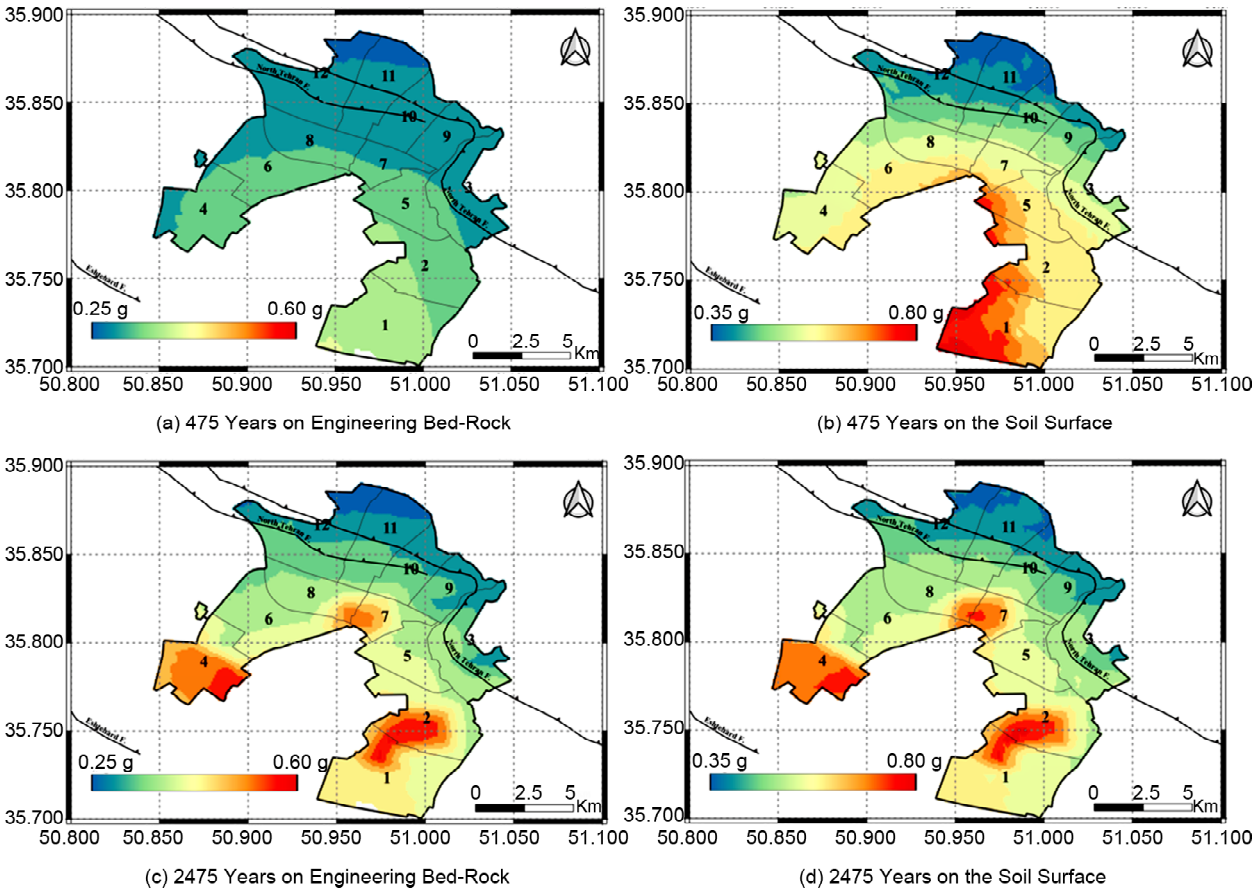

Figure 10. The seismic hazard map of Karaj using event-based approach (PGA) for return periods.

to reach stable results. The seismic hazard map of Karaj for PGA in return periods of 475 and 2475 years on bed-rock and soil surface is shown in Figure 10. There are two interesting differences between the results of the classical PSHA and event-based approaches. Firstly, in the classical PSHA, the ground motion values are higher in the northern parts of Karaj, particularly on bed-rock. While, in the event-based approach, the ground motion values in the southern and central parts of the city are higher. This contradiction related to the difference of these approaches in determining the spatial probability distribution of earthquakes. In the classical PSHA, the spatial probability distribution of earthquakes is determined from defined seismic sources; while, in the event-based approach, the location of synthetic events is used for determining the spatial probability distribution of earthquakes. As illustrated in Figure (2), more earthquakes occurred in the southern parts of the city. These earthquakes in the event-based approach are causes of generation of more synthetic events in the south of Karaj. Thus, the acceleration in the south of Karaj is higher in the event-based approach. Secondly, the ground motion values in the classical approach (Figure 7) are relatively higher compared to event-based; particularly, in return period of 2475 years. The difference of two methods to deal with aleatoric uncertainty of GMPEs is the main response to this disparity. The aleatoric uncertainty is taken into account in the classical PSHA using integration, which is truncated at a fixed number of the logarithmic standard deviation (this value is usually fixed to 3); however, the aleatory uncertainty is taken into account in the event-based approach using random sampling of GMPEs variability.

To clarify the impact of considering aleatory uncertainty on each approach, the hazard curve of a single point in Karaj (Shahrak-e Metro, 35.82N, 50.91E) using the classical approach and event-based approaches is shown in Figure (11). As depicted, in short return periods, the hazard curve of two approaches are relatively similar; however, in long return periods (e.g., more than 2475 years) the event-based methods significantly presents the lower value of PGA. Thus, design of structures

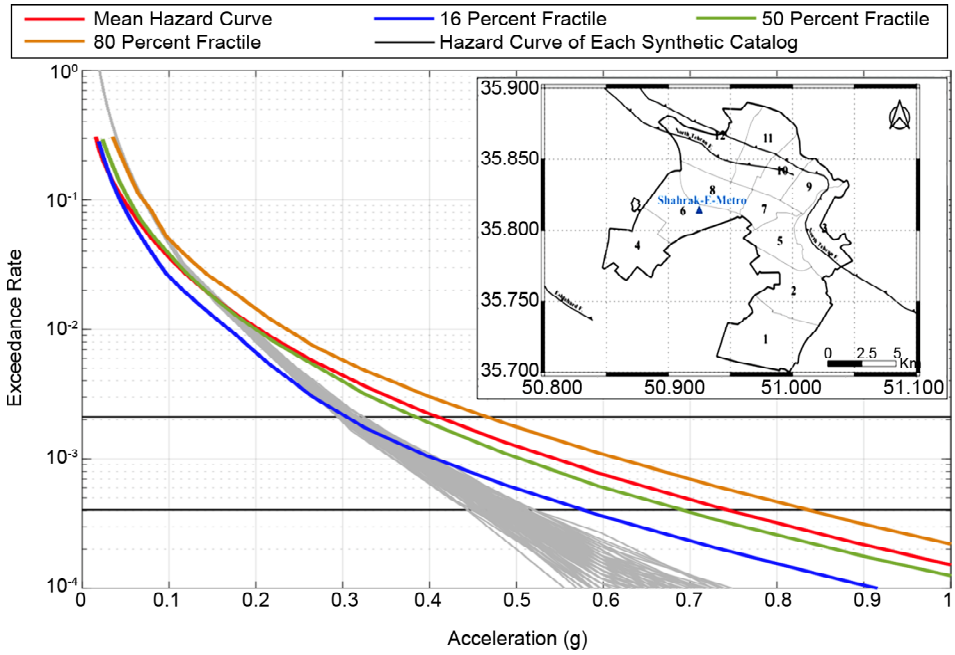

Figure 11. The hazard curves of PGA in specified point (Shahrak-e Metro) within Karaj using the event-based approach (gray lines) and classical method.

such as power plants and nuclear waste storage facilities using the classical PSHA may result in unreasonable values (Wu et al., 2011). Similarly, the computation of Annualized Earthquake Loss (AEL), which is an important parameter for insurance sector to set the premium, using the classical PSHA may provide high value (Firuzi et al., 2019).

6. Ground Motion Shaking Maps of Dominant Seismic Scenarios

The PSHA provides the hazard curve based on the probabilistic methods. These approaches lead to lose of the hazard due to dominant earthquakes, which have the most vulnerability. One of the important outcomes of seismic loss assessment is determining the losses due to catastrophic scenarios. The most challenging issue in this regard is identifying dominant seismic scenarios. Generally, disaggregation analysis is used for determining the contribution of different seismic sources in hazard (Bazzurro & Cornell, 1999). However, this approach provides the contribution of seismic sources for a specific level of ground motion value (e.g., the earthquake with 10% of probability in 50 years). While, it is necessary to identify catastrophic earthquakes with the highest vulnerability. As a result, in this study, a deterministic seismic hazard analysis is performed. The results of the analysis show that the North-Tehran Fault and Eshtehard fault ruptures have the greatest potential for producing the highest acceleration; consequently, the highest vulnerability. Thus, the corresponding ground motion shaking maps of these seismic scenarios are generated. Figure (12) shows the location of these active faults in relation to the Karaj. These line sources have 213 and 63 km length, respectively. Therefore, determining the epicenter of rupture for generating the hazard of the region is a challenge. In the present study, the epicenter of the rupture is randomly selected from the trace of faults. This iteration is performed 1000 times to reach stable results. The iteration is also performed regarding the potential magnitude of the sources. Ritz et al. (2012) by assessing the data of past 30000 years along the North-Tehran fault indicated that this active fault has the potential of generating the magnitude of 6.2-7.2 Mw. This is in accordance of rupture of 50 percent of fault based on the relation of Wells and Coppersmith (1994). By considering similar length of rupture, the Eshtehard fault has the potential of producing magnitude of 6.3-6.7 in the present study; the maximum magnitude in each iteration is randomly from the aforementioned interval in each seismic scenario. The corresponding ground motion shaking maps due to seismic scenarios are shown in Figure (13).

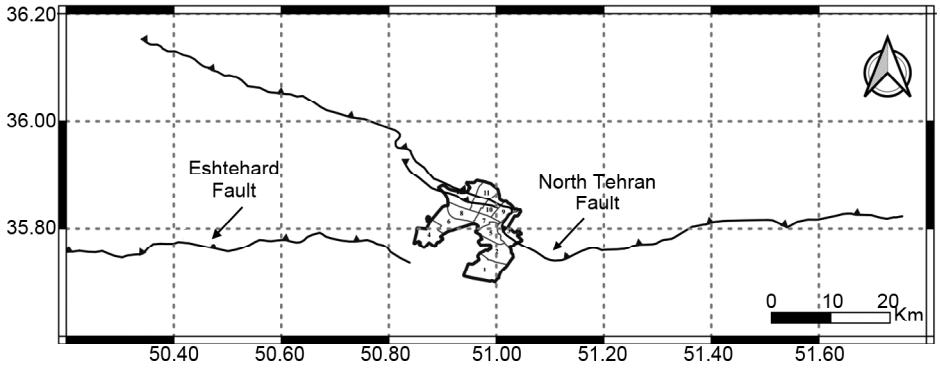

Figure 12. The location of North-Tehran and Eshtehard faults with respect to the Karaj.

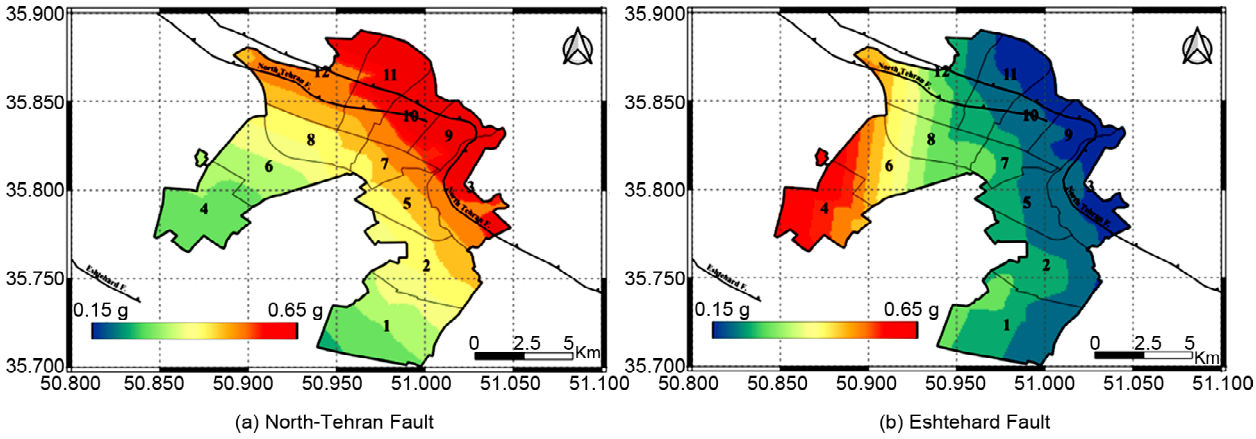

Figure 13. The ground motion shaking map due to rupture.

As depicted, the rupture of the North-Tehran Fault provides the highest acceleration in the northern and central parts of the city. While, the rupture of Eshtehard fault produce the highest acceleration in the southern parts of Karaj. The ground shaking map of seismic scenarios can be used for seismic risk assessment in Karaj.

7. Conclusion

This paper provides a comprehensive process of performing seismic hazard analysis in Karaj. In the present study, two probabilistic approaches, including the classical and event-based methods are used to quantify the seismic hazard in Karaj. The results of two approaches are compared. In this regard, a reliable earthquake catalog of the region is compiled. In addition, two statistical methods including the LH and LLH are used to assess for selecting the most appropriate GMPEs.

To quantify PSHA using the classical approach, a logic tree composed of 360 branches is used. These branches include the uncertainty related to selection of GMPEs, defining seismic sources, declustering the earthquake catalog, determining depth and maximum magnitude of seismic sources. In addition to classical PSHA, the event-based approach is also used to quantify the seismic hazard in Karaj. This is an appropriate approach to handle available uncertainty and subjectivity in the classical method. In this approach, 250 synthetic catalogs with length of 100,000 years are generated. The aleatory uncertainty of GMPEs considered in analysis using the random sampling of inter-event viabilities of GMPEs. The spatial correlation of ground motion values also incorporated in analysis based on the study done by Zafarani et al. (2019).

There are two interesting differences between the results of event-based and classical approaches. First, the event-based approach provides the lower value of PGA in the same return periods in comparison to the classical approach; particularly, in the long return periods. For example, for the return period of 475 years, the event-based and classical respectively provides the PGA around 0.30 g and 035 g. This discrepancy is mainly

related to the different essence of the classical and the event-based approach to deal with aleatory uncertainties. In the classical PSHA, the aleatory uncertainty takes into account using the integration, which is truncated at a fixed number of the logarithmic standard deviation. While, in the Monte Carlo simulation approach, the aleatory uncertainty is considered in calculation using random sampling of GMPEs variability. Second, in the event-based approach, the PGA in the southern parts of the city is higher (the acceleration of both engineering bed-rock and soil surface); while, in the classical approach, the PGA in the northern parts of the city is higher, particularly, the acceleration of bed-rock. This contradiction attributed to the difference of two approaches in quantifying the spatial probability of occurrence of earthquakes. In the classical approach, the spatial probability is determined based on defined seismic sources; while, in the event-based method, the spatial probability is determined based on the region's earthquake catalog. Due to the occurrence of more events in the southern parts of the city, more events in the synthetic catalogs are generated in these regions. Thus, their corresponding acceleration is higher.

Furthermore, the ground motion shaking maps of the city for dominant earthquakes are also developed. The main challenge regarding the probabilistic approach is the loss of dominant earthquake in analysis. Thus, a deterministic analysis is performed to identify the catastrophic events. The analysis shows the ruptures of the North-Tehran and Eshtehard faults have the highest potential of producing significant PGA. It should be remarked to consider the uncertainty related to the epicenter of the rupture in seismic scenarios, a random sampling of epicenter on the fault trance is performed. The results show that the rupture of North-Tehran fault provides the high acceleration (the maximum value around 0.62 g for PGA) in the northern and central parts of the city; while, the rupture of Eshtehard fault provides high acceleration in the southern parts of Karaj (the maximum value around 0.50 g for PGA). These results can be used by engineers for seismic loss estimation to develop appropriate risk mitigation plans in Karaj.

Acknowledgment

The authors gratefully appreciate all those individuals and organizations contributing to the compiling data sets used in the present study, particularly the International Institute of Earthquake Engineering and Seismology (IIEES) for providing the V_{S30} map of Karaj.

References

Abrahamson, N.A., Silva, W.J., & Kamai, R. (2014) Summary of the ASK14 ground motion relation for active crustal regions. *Earthquake Spectra*, *30*(3), 1025-1055.

Ansari, A., Firuzi, E., & Etemadsaeed, L. (2015). Delineation of seismic sources in probabilistic seismic-hazard analysis using fuzzy cluster analysis and Monte Carlo Simulation. *Bulletin of the Seismological Society of America*, *105*(4), 2174-2191.

Ashtari, M., Hatzfeld, D., & Kamalian, N. (2005). Microseismicity in the region of Tehran. *Tectonophysics*, *395*(3-4), 193-208.

Bazzurro, P., & Allin Cornell, C. (1999). Disaggregation of seismic hazard. *Bulletin of the Seismological Society of America*, *89*(2), 501-520.

Beauval, C., Tasan, H., Laurendeau, A., Delavaud, E., Cotton, F., Gueguen, P., & Kuehn, N. (2012) On the testing of ground motion prediction rquations against dmall magnitude fata. *Bulletin of the Seismological Society of America*, *102*(5), 1994-2007.

Berberian, M., & Yeats, R.S. (1999). Patterns of historical earthquake rupture in the Iranian Plateau. *Bulletin of the Seismological Society of America*, *89*(1), 120-139.

Bindi, D., Massa, M., Luzi, L., Ameri, G., Pacor, F., Puglia, R., & Augliera, P. (2014). Pan-european ground-motion prediction equations for the average horizontal component of PGA, PGV, and 5%-damped PSA at spectral periods up to 3.0 s using the RESORCE dataset. *Bulletin of Earthquake Engineering*, *12*(1), 391-430.

Bommer, J.J., Douglas, J., Scherbaum, F., Cotton, F., Bungum, H., & Fallh, D. (2010). On the selection

of ground-motion prediction equations for seismic hazard analysis. *Seismological Research Letters*, *81*(5), 783-793.

Bommer, J.J., Scherbaum, F., Bungum, H., Cotton, F., Sabetta, F., & Abrahamson, N.A. (2005). On the use of logic trees for ground-motion prediction equations in seismic-hazard analysis. *Bulletin of the Seismological Society of America*, *95*(2), 377-389.

Boore, D.M., Stewart, J.P., Seyhan, E., & Atkinson, G.M. (2014) NGA-West2 equations for predicting PGA, PGV, and 5% damped PSA for shallow crustal earthquakes. *Earthquake Spectra*, *30*(3), 1057-1085.

Campbell, K.W., & Bozorgnia, Y. (2014). NGA-West2 ground motion model for the average horizontal components of PGA, PGV, and 5% damped linear acceleration response spectra. *Earthquake Spectra*, *30*(3), 1087-1115.

Chiou, B.S.J., & Youngs, R.R. (2014). Update of the Chiou and Youngs NGA model for the average horizontal component of peak ground motion and response spectra. *Earthquake Spectra*, *30*(3), 1117-1153.

Cornell, C.A. (1968). Engineering seismic risk analysis. *Bulletin of the Seismological Society of America*, *58*(5), 1583-1606.

Cotton, F., Scherbaum, F., Bommer, J.J., & Bungum, H. (2006) Criteria for selecting and adjusting ground-motion models for specific target regions: application to central europe and rock sites. *Journal of Seismology*, *10*(2), 137-156.

Crowley, H. (2014). Earthquake risk assessment: present shortcomings and future directions. In Perspectives on European Earthquake Engineering and Seismology, 515-532, Springer, Cham.

Crowley, H., & Bommer, J.J. (2006). Modelling seismic hazard in earthquake loss models with spatially distributed exposure. *Bulletin of Earthquake Engineering*, *4*(3), 249-273.

Danciu, L., Kale, O., & Akkar, S. (2018). The 2014 earthquake model of the middle east: ground motion model and uncertainties. *Bulletin of Earthquake Engineering*, *16*(8), 3497-3533.

Ebel, J.E., & Kafka, A.L. (1999). A Monte Carlo approach to seismic hazard analysis. *Bulletin of the Seismological Society of America*, *89*(4), 854-866.

Fallah Tafti, M., Amini Hosseini, K., Firouzi, E., Mansouri, B., & Ansari, A. (2017). Ranking of GMPEs for seismic hazard analysis in Iran using LH, LLH and EDR approaches. *Journal of Seismology and Earthquake Engineering*, *19*(2), 139-161.

Farajpour, Z., Pezeshk, S., & Zare, M. (2019). A new empirical ground-motion model for Iran. *Bulletin of the Seismological Society of America*, *109*(2), 732-744.

Firuzi, E., Ansari, A., Amini Hosseini, K., & Karkooti, E. (2020). Developing a customized system for generating near real time ground motion ShakeMap of Iran's earthquakes. *Journal of Earthquake Engineering*, 1-23.

Firuzi, E., Ansari, A., Hosseini, K.A., & Rashidabadi, M. (2019). Probabilistic earthquake loss model for residential buildings in Tehran, Iran to quantify annualized earthquake loss. *Bulletin of Earthquake Engineering*, *17*(5), 2383-2406.

Gardner, J. K., & Knopoff, L. (1974). Is the sequence of earthquakes in Southern California, with aftershocks removed, Poissonian. *Bulletin of the Seismological Society of America*, *64*(5), 1363-1367.

Ghasemi, H., Zare, M., Fukushima, Y., & Sinaeian, F. (2009). Applying empirical methods in site classification, using response spectral aatio (H/V): A case study on Iranian Strong Motion Network (ISMN). *Soil Dynamics and Earthquake Engineering*, *29*(1), 121-132.

Gutenberg, B., & Richter, C.F. (1944). Frequency of earthquakes in California. *Bulletin of the Seismological society of America*, *34*(4), 185-188.

Han, S.W., & Choi, Y.S. (2008). Seismic hazard analysis in low and moderate seismic region-Korean peninsula. *Structural Safety*, *30*(6), 543-558.

Idriss, I.M. (2014). An NGA-West2 empirical model for rstimating the horizontal spectral values generated by shallow crustal earthquakes. *Earth-*

quake Spectra, *30*(3), 1155-1177.

IIEES (International Institute of Earthquake Engineering and Seismology) (2013). *The Micro-Zonation Study of Karaj* (in Persian).

Jackson, J., Priestley, K., Allen, M., & Berberian, M. (2000). Active tectonics of the South Caspian basin. *Geophys. J. Int.*, *148*, 214-245.

Jalalalhosseini, S. M., Zafarani, H., & Zare, M. (2018). Time-dependent seismic hazard analysis for the Greater Tehran and surrounding areas. *Journal of Seismology*, *22*(1), 187-215.

Jarahi, H. (2016). Probabilistic seismic hazard deaggregation for Karaj City (Iran). *Am. J. Eng. Applied Sci.*, *9*, 520-529.

Kale, O., Akkar, S., Ansari, A., & Hamzehloo, H. (2015). A ground motion predictive model for Iran and Turkey for horizontal PGA, PGV, and 5% damped response spectrum: investigation of possible regional effects. *Bulletin of the Seismological Society of America*, *105*(2A), 963-980.

Khodaverdian, A., Zafarani, H., Rahimian, M., & Dehnamaki, V. (2016). Seismicity parameters and spatially smoothed seismicity model for Iran. *Bulletin of the Seismological Society of America*, *106*(3), 1133-1150.

Kijko, A., & Sellevoll, M.A. (1992). Estimation of earthquake hazard parameters from incomplete data files. Part II. Incorporation of magnitude heterogeneity. *Bulletin of the Seismological Society of America*, *82*(1), 120-134.

Kotha, S.R., Bindi, D., & Cotton, F. (2016). Partially non-ergodic region specific GMPE for Europe and middle-east. *Bulletin of Earthquake Engineering*, *14*(4), 1245-1263.

Mirzaei, N., Mengtan, G., & Yuntai, C. (1998). Seismic source regionalization for seismic zoning of Iran: major seismotectonic provinces. *Journal of Earthquake Prediction Research*, *7*, 465-495.

Mousavi, M., Ansari, A., Zafarani, H., & Azarbakht, A. (2012). Selection of ground motion prediction models for seismic hazard analysis in the Zagros region, Iran. *Journal of Earthquake Engineering*, *16*(8), 1184-1207.

Mousavi-Bafrouei, S.H., & Mahani, A.B. (2020). A comprehensive earthquake catalogue for the Iranian Plateau (400 BC to December 31, 2018). *Journal of Seismology*, *24*, 709-724.

Musson, R.M. (2000). *The Use of Monte Carlo Simulations for Seismic Hazard Assessment in the UK*.

Pagani, M., Monelli, D., Weatherill, G., Danciu, L., Crowley, H., Silva, V., ... & Vigano, D. (2014). OpenQuake engine: An open hazard (and risk) software for the global earthquake model. *Seismological Research Letters*, *85*(3), 692-702.

Reasenberg, P. (1985). Second-order moment of central California seismicity, 1969-1982. *Journal of Geophysical Research: Solid Earth*, **90**(B7), 5479-5495.

Ritz, J. F., Nazari, H., Balescu, S., Lamothe, M., Salamati, R., Ghassemi, A., ... & Saidi, A. (2012). Paleoearthquakes of the past 30,000 years along the North Tehran Fault (Iran). *Journal of Geophysical Research: Solid Earth*, *117*(B6).

Scherbaum, F., Cotton, F., & Smith, P. (2004). On the use of response spectral-reference data for the selection and ranking of ground-motion models for seismic-hazard analysis in regions of moderate seismicity: the case of rock motion. *Bulletin of the Seismological Society of America*, *94*(6), 2164-2185.

Scherbaum, F., Delavaud, E., & Riggelsen, C. (2009). Model selection in seismic hazard analysis: an information-theoretic perspective. *Bulletin of the Seismological Society of America*, *99*(6), 3234-3247.

Silva, V. (2017). Critical issues on probabilistic earthquake loss assessment. *Journal of Earthquake Engineering*, *22*(9), 1683-1709.

Statistical Centre of Iran (SCI), 1956-2016, Statistical Centre of Iran, Vice-Presidency for Strategic Planning and Supervision, Tehran, National Census of Population and Housing Technical Reports, Sarshomari 2016 (1395), 2011 (1390), 2006 (1385), 1996 (1375), 1986 (1365), and 1976 (1355): Tehran, SCI, formerly, the Plan & Budget Organization of the Imperial Government of Iran, Statistical Centre,

http://www.amar.org.ir/Default.aspx?tabid=116 (accessed 2018).

Wald, D.J., & Allen, T.I. (2007). Topographic slope as a proxy for seismic site conditions and amplification. *Bulletin of the Seismological Society of America*, *97*(5), 1379-1395.

Wells, D.L., & Coppersmith, K.J. (1994). New empirical relationships among magnitude, rupture length, rupture width, rupture area, and surface displacement. *Bulletin of the seismological Society of America*, *84*(4), 974-1002.

Wiemer, S. (2001). A software package to analyze seismicity: ZMAP. *Seismological Research Letters*, *72*, 374-383.

Wu, J., Gao, M., Chen, K., & Huang, B. (2011). Discussion on the influence of truncation of ground motion residual distribution on probabilistic seismic hazard assessment. *Earthquake Engineering and Engineering Vibration*, *10*(3), 379-392.

Zafarani, H., & Mousavi, M. (2014). Applicability of different ground-motion prediction models for northern Iran. *Natural Hazards*, *73*(3), 1199-1228.

Zafarani, H., & Soghrat, M.R. (2017). A selected dataset of the Iranian strong motion records. *Natural Hazards*, *86*(3), 1307-1332.

Zafarani, H., Ghafoori, S.M.M., Soghrat, M., & Shafiee, M. (2019). Spatial correlation of peak ground motions and pseudo-spectral acceleration based on the sarpol-e Zahab Mw 7.3, 2017 earthquake data. *Annals of Geophysics*, *63*(4), SE439-SE439.

Zafarani, H., Ghafoori, S.M.M., & Adlaparvar, M.R. (2021). Spatial correlation of peak ground motions and pseudo spectral acceleration based on the Iranian multievent datasets. *Journal of Earthquake Engineering*, 1-21.

Zaman, M., & Ghayamghamian, M. R. (2021). *Risk-Adjusted Design Basis Earthquake's Adequacy for use in Seismic Design Codes*.